DOI: 10.1002/ange.201107145

Heterogeneous Catalysis

Catalytic Polymerization of Anthracene in a Recyclable SBA-15 Reactor with High Iron Content by a Friedel–Crafts Alkylation**

Jeonghun Kim, Chokkalingam Anand, Siddulu N. Talapaneni, Jungmok You, Salem S. Aldeyab, Eunkyoung Kim, and Ajayan Vinu**

Mesoporous materials that contain metallosilicate frameworks have been receiving considerable attention in recent years because of their excellent texture characteristics. These properties include high specific surface area, large pore volume, and well-ordered pores that are significantly larger than in microporous aluminosilicate and aluminophosphate molecular sieves. Such materials are remarkably active as catalysts for various acid-catalyzed transformations, such as Friedel–Crafts acylation, alkylation, cracking, and isomerization.[1–9] The well-ordered mesopores and the high surface area of these materials allow the reactant or adsorbate molecules to access the active sites without any diffusion limitation, and can also dictate the efficiency of the catalyst in organic transformations. Despite these interesting properties, these materials have not yet been extensively utilized for the transformation of bulky molecules, which includes polymerization into high molecular weight (M_w) polymers. Lin et al. reported the synthesis of a conjugated polymer through an oxidative polymerization of 1,4-diethynylbenzene by using the Cu-substituted mesoporous silica MCM-41.[9] Although the polymeric materials were prepared by using this catalyst, unfortunately the average molecular weight of the resultant polymer was small. The mesostructure of the catalyst completely collapsed after the polymerization process and the broken silica particles remained as an impurity in the final product. The smaller pore diameter and the low amount of Cu in the wall structure of MCM-41 are responsible for its poor activity, whereas a thin wall and a weak mechanical stability caused the collapse of the structure after the polymerization. In addition, it is extremely difficult to prepare an MCM-41-type material with a high copper content, an ultralarge pore diameter, and thick walls without affecting the mesoporous structure. These drawbacks hinder the efficient use of these metal-substituted MCM-41 materials for the synthesis of polymers with high molecular weights.

SBA-15 is a material which has a hexagonally ordered porous structure and has thicker pore walls, as well as better mechanical, thermal, and solvent stabilities than MCM-41.[10] However, the incorporation of metal species into the silica framework, which is generally neutral and does not provide any acidic or redox-active sites, is extremely difficult because the preparation of such materials requires a highly acidic medium, in which the solubility of the metal species is very high. Recently, Vinu et al. reported a novel method for incorporating metal species in a silica framework by tuning the water to the hydrochloric acid molar ratio of the synthesis gel.[2a] However, the amount of the metal in the final product is less than that added in the synthesis gel. Herein, we demonstrate the preparation of Fe-substituted SBA-15 with an extremely high Fe content and a large pore diameter. To produce this material we combine a pH-adjusting method and a high temperature technique to simultaneously control the Fe content as well as the pore diameter of the final product.

We have previously reported the polymerization of anthracene in the presence of chloromethyl methyl ether (CME) by using $FeCl_3$ as a catalyst through a simple Friedel–Crafts reaction.[11] The resulting poly(methylene anthracene) (PMAn) was highly fluorescent and photopatternable, and can be used for the fabrication of organic displays.[11,12] However, the use of the homogenous catalyst has several disadvantages, such as toxicity, handling hazards, difficulty in separating and recovering the catalyst, isolation of the product, and the formation of a large amount of waste. These drawbacks limit the commercialization of the process and push researchers to find an alternative synthesis strategy. Herein, we also report the catalytic polymerization of anthracene inside the nanochannels of Fe-substituted SBA-15 that has a large pore diameter. As the polymerization is initiated with the help of the Fe centers in the silica walls and the polymers are formed inside the nanochannels (Figure 1), we have fabricated SBA-15 with different Fe contents and pore diameters to control the polymerization process.

FeSBA-15 materials were prepared by mixing Pluronic P123 and tetraethyl orthosilicate in the presence of ferric nitrate, and subsequent calcination at 540 °C as described in the Supporting Information. The amount of Fe and the pore

[*] Dr. C. Anand, S. N. Talapaneni, Prof. A. Vinu
International Center for Materials Nanoarchitectonics
National Institute for Materials Science
1-1 Namiki, Tsukuba 305-0044, Ibaraki (Japan)
J. Kim, Dr. J. You, Prof. E. Kim
Department of Chemical and Biomolecular Engineering
Yonsei University, Seoul 120-749 (Korea)
E-mail: eunkim@yonsei.kr
Dr. C. Anand, Prof. A. Vinu
Australian Institute for Bioengineering and Nanotechnology
University of Queensland, Brisbane 4072, Queensland (Australia)
E-mail: a.vinu@uq.edu.au
Prof. S. S. Aldeyab
Department of Chemistry, Faculty of Science
King Saud University, Riyadh (Kingdom of Saudi Arabia)

[**] This work was supported financially by the MEXT (Japan) and KSU, Saudi Arabia. J.K. thanks NIMS for an I.J.G.S. Fellowship. E.K. acknowledges financial support from the Korean government (MEST) through the Active Polymer Center for Pattern Integration (No. R11-2007-050-00000-0) and the Seoul R&BD Program (10816).
Supporting information for this article is available on the WWW under http://dx.doi.org/10.1002/anie.201107145.

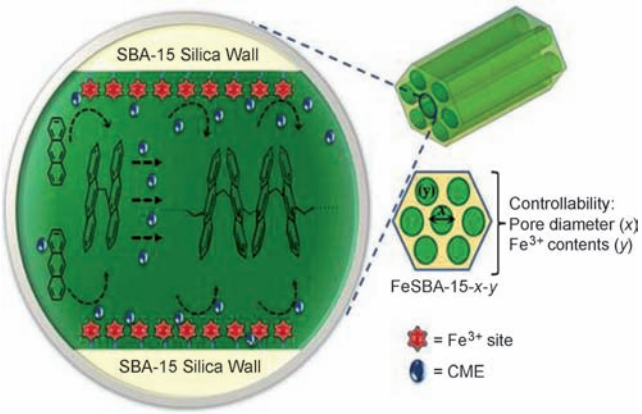

Figure 1. Representation of Fe^{+3} incorporated into mesoporous silica (FeSBA-15-*x*-*y*) catalysts for the catalytic polymerization of anthracene into the highly fluorescent functional polymer PMAn with a high molecular weight by a Friedel–Crafts alkylation. CME = chloromethyl methyl ether.

diameter of the FeSBA-15 materials were varied by adjusting the synthesis temperature. The catalysts are denoted FeSBA-15-*x*-*y*, where *x* and *y* are the synthesis temperature of the FeSBA-15 and the n_{Si}/n_{Fe} molar ratio, respectively. Elemental analysis showed that the amount of Fe in the samples that were prepared at 130 °C and 150 °C is much higher than in the sample that was prepared at 100 °C, which revealed that a high-temperature synthesis favors the incorporation of more Fe into the silica framework (Table S1 in the Supporting Information).

The powder XRD patterns of samples of FeSBA-15 with $n_{Si}/n_{Fe} = 2$ that were prepared at different temperatures are shown in Figure 2. The XRD patterns of all of the FeSBA-15 materials have a sharp peak at a lower angle and several well-resolved, higher order peaks that can be indexed to the (100), (110), and (200) reflections of the hexagonal space group P6mm. These well-defined patterns are similar to those of the highly ordered pure SBA-15 that has a hexagonal porous structure, which was prepared by Zhao et al.[10] These patterns confirm the well-ordered nature of the materials. Interestingly, the structures of the FeSBA-15 samples that have different n_{Si}/n_{Fe} ratios and were prepared at different temperatures are also highly ordered, which was confirmed by the presence of well-resolved (100), (110) and, (200) reflections at a lower angle. The presence of incorporated Fe was also demonstrated (Figures S1–S4 and Table S1 in the Supporting Information). It should be noted that the unit-cell constant of the FeSBA-15 samples decreased with an increase in Fe content in the sample that was prepared at 100 °C. On the other hand, the peaks are shifted towards the lower angle region with increasing synthesis temperature, which results in a significant increase in the unit-cell constant of the samples that were prepared at higher temperature (Table S1 in the Supporting Information). These results indicate that the structural properties of the material depend on the Fe content and the synthesis temperature. The structure and the Fe content can be easily controlled by adjusting the reaction temperature.

The texture of the materials was also significantly affected by the synthesis temperature and the amount of Fe in the silica framework of SBA-15 (Figure 3, see also Figure S5 in the Supporting Information). All of the samples have a type IV adsorption isotherm, which is typical for this type of mesoporous material. This finding reveals that the mesoporous structure is retained in all of the samples, even after the incorporation of huge amount of Fe. Increasing the synthesis temperature from 100 °C to 150 °C resulted in the specific surface area of the samples decreasing from

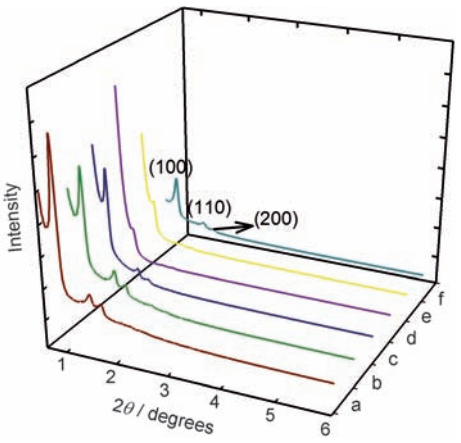

Figure 2. Powder X-ray diffraction patterns of unused FeSBA-15-*x*-2 prepared at different temperature: a) *x* = 100, b) *x* = 130, c) *x* = 150, and recovered FeSBA-15-*x*-2 after polymerizations d) *x* = 100, e) *x* = 130, f) *x* = 150.

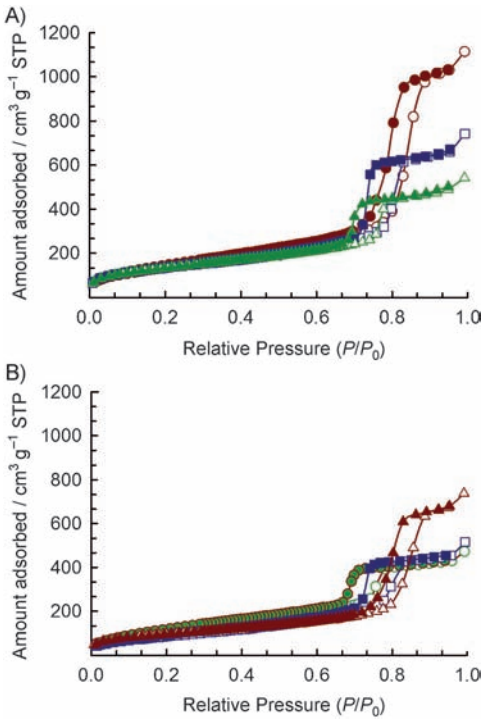

Figure 3. N_2 adsorption/desorption isotherms of FeSBA-15-100-2 (green), FeSBA-15-130-2 (blue), and FeSBA-15-150-2 (red). A) Before and B) After PMAn polymerization for 60 h. Adsorption: closed symbols; desorption: open symbols.

Table 1: Catalysts used and the results of catalytic polymerizations of anthracene.

Entry	Catalyst	Surface area [$m^2 g^{-1}$]	Pore size [nm]	Pore volume [$cm^3 g^{-1}$]	Catalyst content [wt%][a]	Temperature[b] [°C]	M_w [$g mol^{-1}$]	Yield [%] [c]
R1	FeSBA-15-100-2	710	9.2	0.90	2.5	45	4300	90
R2	FeSBA-15-130-2	485	11.4	1.02	2.5	25	2500	65
R3	FeSBA-15-130-2	485	11.4	1.02	2.5	45	8500	93
R4	FeSBA-15-130-2	485	11.4	1.02	5	45	9700	67[d]
R5	FeSBA-15-130-2	485	11.4	1.02	10	45	-[e]	-[e]
R6	FeSBA-15-150-2	514	13.5	1.79	2.5	45	3200	86

[a] Catalyst content: wt% with respect to the monomers. [b] Polymerization temperature. [c] Yield of isolated product. [d] Yield after removal of insoluble byproducts. [e] Insoluble products.

710 $m^2 g^{-1}$ to 514 $m^2 g^{-1}$, whereas the specific pore volume and the pore diameter increased from 0.90 $cm^3 g^{-1}$ to 1.79 $cm^3 g^{-1}$ and from 9.2 nm to 13.5 nm, respectively (Table 1). All of the samples have a narrow pore size distribution, except for the sample that was prepared at 150 °C, which has a broad pore size distribution (Figure S4 in the Supporting Information). Therefore, the structural order of FeSBA-15-150-2 was not as good as that of FeSBA-15-130-2 and FeSBA-15-100-2.

These novel FeSBA-15 materials that have different pore diameters and Fe contents were used for the catalytic polymerization of anthracene inside the nanopore (Figure 1). FeSBA-15 catalysts (2.5–10 wt% with respect to anthracene) were added to the mixture of CME and anthracene in a solution of chloroform under N_2. The detailed experimental procedure is given in the experimental section. In general, the reaction was carried out at 45 °C. After the reaction, the catalyst was removed by filtration and the polymer product was recrystallized from methanol to give highly fluorescent and soluble PMAn in a high yield. The yield of the polymerization was highly sensitive to the Fe content in the catalyst. The yield was less than 50% when the Fe content was low ($y = 5$ or 7). However, the yield increased to more than 90% when $n_{Si}/n_{Fe} = 2$, which indicates that Fe is the active site for polymerization. Of the catalysts studied, FeSBA-15-130-2 had the highest activity. The reaction with FeSBA-15-130-2 afforded the highest yield of PMAn with a high molecular weight, although FeSBA-15-150-2 has the largest pore diameter. This could be because of the well-ordered mesoporous structure together with the large pore diameter and pore volume of FeSBA-15-130-2 relative to the broad pore size distribution and the slightly distorted mesoporous structure caused by the high temperature synthesis of FeSBA-15-150-2.

The reaction temperature and the weight of the catalyst play a critical role in controlling the yield and the molecular weight of the product. When the reaction temperature was 25 °C, the yield and molecular weight of PMAn were as low as 65% and 2500, respectively (Table 1, entry R2), but the yield and molecular weight increased to 93% and 8500, respectively, when the reaction temperature was 45 °C. On the other hand, the molecular weight of PMAn was higher but the yield was lower when more than 2.5 wt% of the catalyst was used in the reaction (Table 1, entry R4). When the amount of catalyst was increased to approximately 10 wt%, the reaction afforded insoluble dark brown particles (Table 1, entry R5), possibly because of an oxidative polymerization of anthracene that results in insoluble polymers with a high molecular weight. It should also be noted that the PMAn that was produced in most of the reactions catalyzed by FeSBA-15 was soluble in many different organic solvents, and that films of PMAn were also successfully fabricated. The PMAn solutions as well as the thin films that were prepared from the solution were highly fluorescent. To our knowledge, the use of mesoporous materials that were directly synthesized in a highly acidic medium and have a high metal content as well as ultra large pores to synthesize functional polymers in powder and film forms has not been reported.

To check the stability of the catalysts for reuse, the catalysts that were recovered from the reactions were collected and characterized by XRD as well as N_2 adsorption measurements. These analyses revealed that the structure of the catalysts was preserved even after the polymerization process (Figure 2 and Figure 3, see also Figure S5 and Table S2 in the Supporting Information). As can be seen in Figure 3 and Figure S5, the amount of N_2 that was adsorbed by the recovered catalysts is much lower than that of the unused catalysts because of residual polymers inside the nanochannels. These results confirm that the active Fe centers catalyze the reaction, and that the mesopores help the formation of polymers with a high molecular weight. Furthermore, the recovered catalyst was washed several times and heated at high temperature to remove the residual polymers from the nanochannels. Interestingly, the weight of the catalyst that was recovered from each of the reactions after washing and the heat treatment is almost same as that added to each reaction, which demonstrates that the PMAn was not contaminated with the FeSBA-15 catalysts, and that the iron or iron oxide active centers were not leached out from the FeSBA-15. These results further confirm that the catalysts are highly stable and can be reused several times without affecting the structure or the texture of the catalysts.

The optical properties of the PMAns were also investigated. The absorbance and emission maxima of PMAn were red-shifted relative to those of pure anthracene (Figure 4), but were comparable to the PMAn that was synthesized under homogeneous conditions by using $FeCl_3$, at the same concentration of anthracene unit.[11] Although only to a small extent, the absorption and emission maxima were red-shifted as the molecular weight of PMAn increased (Table S3 in the Supporting Information). The fluorescence quantum yield (Φ_E) of the polymers was between 29–74%, depending on the molecular weight of PMAn, as determined by using anthra-

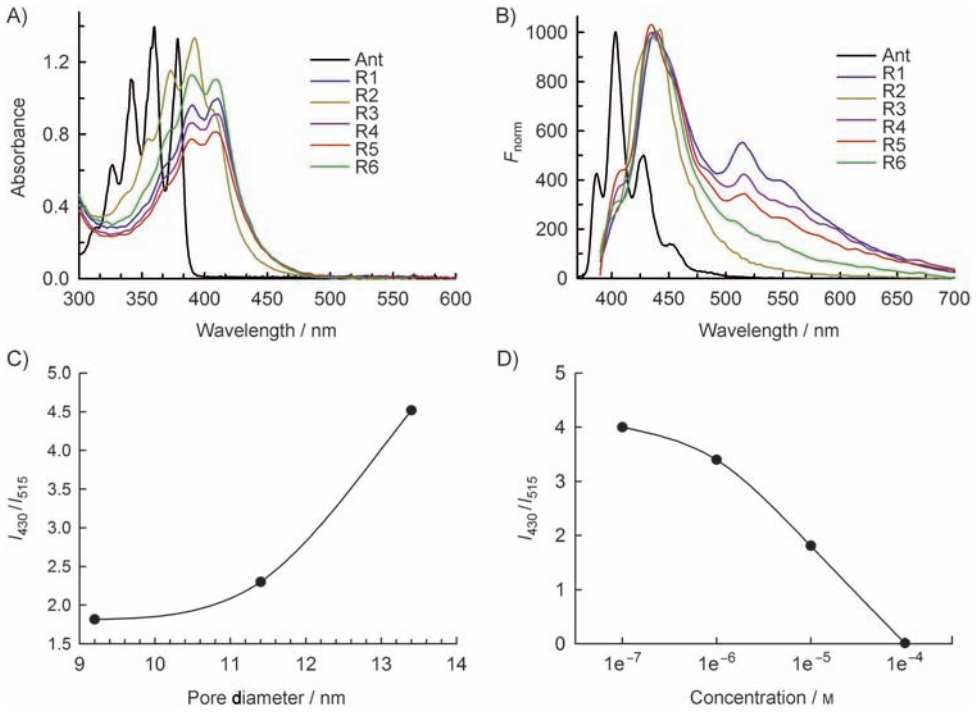

Figure 4. A) Normalized UV-Vis and B) Fluorescence emission (excited at 370 nm) spectra of anthracene (Ant) and PMAn from the reactions R1–R6 in Table 1 in chloroform solution (10^{-5} M). C) Plot of the emission intensity ratio at 430 nm and 515 nm against pore size of the nanoreactor Fe(2)SBA-15(y). D) Plot of the emission intensity ratio at 430 nm and 515 nm against solution concentration (10^{-4}–10^{-7} M) of PMAn obtained from reaction R1 in Table 1.

cene ($\Phi_E = 29\%$) as a reference. The PMAn with a low molecular weight ($M_w = 2500$) had the highest Φ_E value of 74% without anthracene excimer emission, possibly because of a low concentration quenching effect. It is interesting to note that an intense anthracene excimer emission centered at 515 nm was detected for high molecular weight PMAn.[13] As can be seen in Figure 4C, the pore size of the catalyst significantly affects the anthracene excimer emission. The excimer emission may be more favorable if the anthracene molecules are bound close together, which would enhance anthracene–anthracene (A-A) interactions.[14] If polymerization takes place in a nanoreactor with smaller pore sizes, structures with more A-A interactions may be generated as a result of the close arrangement of the molecules. In contrast, if the polymerization takes place in a matrix with large pores, thermodynamically more stable structures with less A-A interactions may be generated. The extreme case would be for the PMAn that is produced under homogeneous reaction conditions with $FeCl_3$, where there is no nanoreactor and the molecules are formed in an open planar surface. A highly intense excimer emission was detected when the concentration of PMAn was high, which is mainly a result of the favorable A-A interaction at higher concentrations (Figure 4D). Further studies on the excited dynamics and the structure of PMAn are required to clarify this interesting issue. However, the relationship between the pore size of the catalyst and the intensity of excimer emission is clear. This finding further confirms that the FeSBA-15 catalyst as well as the nanopore reactor promotes the polymerization reaction, and the polymerization indeed occurs inside the nanochannels of the catalyst. Furthermore this result promises a convenient method for controlling the structure of the product by tuning the pore size and the Fe content of the FeSBA-15 catalysts.

In summary, we have demonstrated for that a FeSBA-15 catalyst with a high Fe content and a large pore diameter can be employed as a highly active and reusable catalyst for the synthesis of highly fluorescent and soluble PMAn with different molecular weights. We also demonstrated that the yield, molecular weight, structure, and optical properties of PMAn can be controlled by tuning the specific surface area, pore diameter, pore volume, and the Fe content of the catalysts. The pore size of the catalyst with a high Fe content was critical to control the emission properties of the resultant polymer, and the polymer that was synthesized by using the catalyst with the smallest pore diameter gives a strong excimer emission. Importantly, the catalyst is highly stable and recyclable. We believe that these highly reactive catalytic systems offer a platform for the development of a series of functional polymers that have exciting and tunable optical properties. Such materials could find applications in various fields, which include sensing, drug delivery, adsorption, catalysis, and optoelectronic nanodevices.

Experimental Section

Preparation of FeSBA-15 catalysts:[8a] FeSBA-15 materials with various Fe^{3+} content and pore diameters were prepared by using the procedure given in the Supporting Information. The molar composition of the gel synthesis mixture was 1:0.143–0.5:0.016:0.46:127 = TEOS/Fe_2O_3/P123/HCl/H_2O.

Synthesis of poly(methylene anthracene) from catalysts: FeSBA-15 catalysts were used for catalytic polymerization, the details of which are given in the Supporting Information. The prepared polymer and the used catalysts were characterized by several techniques, such as XRD, N_2 adsorption, and ^{1}H NMR spectroscopy. ^{1}H NMR ($CDCl_3$): $\delta = 4.22$ (s, CH_2, between anthracene, 2H), 7.4–8.54 ppm (m, anthracene, 8H).[10a]

Received: October 9, 2011
Revised: December 12, 2011
Published online: January 2, 2012

Keywords: Friedel–Crafts alkylation · heterogeneous catalysis · mesoporous materials · polyanthracenes · polymerization

[1] a) N. He, S. Bao, Q. Xu, *Appl. Catal. A* **1998**, *169*, 29; b) A. Tuel, I. Acron, J. M. M. Millet, *J. Chem. Soc. Faraday Trans.* **1998**, *94*, 3501; c) A. Tuel, S. Gontier, *Chem. Mater.* **1996**, *8*, 114; d) A. Corma, V. Fornes, M. T. Navarro, J. Pérez-Pariente, *J. Catal.* **1994**, *148*, 569.

[2] a) A. Vinu, V. Murugesan, W. Böhlmann, M. Hartmann, *J. Phys. Chem. B* **2004**, *108*, 11496; b) A. Vinu, V. Murugesan, M. Hartmann, *J. Phys. Chem. B* **2004**, *108*, 7323; c) A. Vinu, V. Murugesan, O. Tangermann, M. Hartmann, *Chem. Mater.* **2004**, *16*, 3056; d) A. Vinu, M. Hartmann, *Chem. Lett.* **2004**, *33*, 588.

[3] a) A. Vinu, K. Usha Nandhini, V. Murugesan, W. Böhlmann, V. Umamaheswari, A. Pöppl, M. Hartmann, *Appl. Catal. A* **2004**, *265*, 1; b) A. Vinu, T. Krithiga, V. Murugesan, M. Hartmann, *Adv. Mater.* **2004**, *16*, 1817.

[4] a) M. A. Chari, A. Mano, S. T. Selvan, K. Mukkanti, A. Vinu, *Tetrahedron* **2009**, *65*, 10608; b) A. Vinu, P. Kalita, V. V. Balasubramanian, H. Oveisi, T. Selvan, A. Mano, M. A. Chari, B. V. Subba Reddy, *Tetrahedron Lett.* **2009**, *50*, 7132; c) N. Lucas, A. Bordoloi, A. P. Amrute, P. Kasinathan, A. Vinu, W. Bohringer, J. C. Q. Fletcher, S. B. Halligudi, *Appl. Catal. A* **2009**, *352*, 74; d) V. V. Balasubramanian, C. Anand, R. R. Pal, T. Mori, W. Böhlmann, K. Ariga, A. Vinu, *Microporous Mesoporous Mater.* **2009**, *121*, 18.

[5] a) R. Chakravarti, P. Kalita, R. R. Pal, S. B. Halligudi, M. Lakshmi Kantam, A. Vinu, *Microporous Mesoporous Mater.* **2009**, *123*, 338; b) R. Brzozowski, A. Vinu, *Top. Catal.* **2009**, *52*, 1001; c) A. Vinu, J. Justus, C. Anand, D. P. Sawant, K. Ariga, T. Mori, P. Srinivasu, V. V. Balasubramanian, S. Velmathi, S. Alam, *Microporous Mesoporous Mater.* **2008**, *116*, 108; d) R. Brzozowski, A. Vinu, *Stud. Surf. Sci. Catal.* **2008**, *174*, 1299.

[6] a) R. Brzozowski, A. Vinu, T. Mori, *Catal. Commun.* **2007**, *8*, 1681; b) A. Vinu, P. Srinivasu, M. Miyahara, K. Ariga, *J. Phys. Chem. B* **2006**, *110*, 801; c) A. Vinu, B. M. Devassy, S. B. Halligudi, W. Bohlmann, M. Hartmann, *Appl. Catal. A* **2005**, *281*, 207; d) T. Krithiga, A. Vinu, K. Ariga, B. Arabindoo, M. Palanichamy, V. Murugesan, *J. Mol. Catal. A* **2005**, *237*, 238.

[7] a) A. Vinu, J. Dědeček, V. Murugesan, M. Hartmann, *Chem. Mater.* **2002**, *14*, 2433; b) M. Hartmann, A. Vinu, S. P. Elangovan, V. Murugesan, W. Böhlmann, *Chem. Commun.* **2002**, 1238; c) C. Anand, P. Srinivasu, S. Alam, V. V. Balasubramanian, D. P. Sawant, M. Palanichamy, V. Murugesan, A. Vinu, *Microporous Mesoporous Mater.* **2008**, *111*, 72; d) A. Vinu, T. Krithiga, N. Gokulakrishnan, P. Srinivasu, S. Anandan, K. Ariga, T. Mori, V. Murugesan, V. V. Balasubramanian, *Microporous Mesoporous Mater.* **2007**, *100*, 87.

[8] a) A. Vinu, D. P. Sawant, K. Z. Hossain, K. Ariga, S. B. Halligudi, M. Hartmann, *Chem. Mater.* **2005**, *17*, 5339; b) A. Vinu, G. Chandrasekar, M. Hartmann, K. Ariga, *Stud. Surf. Sci. Catal.* **2005**, *156*, 703.

[9] V. Lin, D. Radu, M. Han, W. Deng, S. Kuroki, B. Shanks, M. Pruski, *J. Am. Chem. Soc.* **2002**, *124*, 9040.

[10] D. Zhao, Q. Huo, J. Feng, B. F. Chmelka, G. D. Stucky, *J. Am. Chem. Soc.* **1998**, *120*, 6024.

[11] a) K. Rameshbabu, Y. Kim, T. Kwon, J. Yoo, E. Kim, *Tetrahedron Lett.* **2007**, *48*, 4755; b) J. You, Y. Kim, E. Kim, *Mol. Cryst. Liq. Cryst.* **2010**, *520*, 128.

[12] V. Sinigersky, K. Mullen, M. Klapper, I. Schopov, *Adv. Mater.* **2000**, *12*, 1058.

[13] L. S. Kaanumalle, C. L. D. Gibb, B. C. Gibb, V. Ramamurthy, *J. Am. Chem. Soc.* **2005**, *127*, 3674.

[14] G. Zhang, G. Yang, S. Wang, Q. Chen, J. S. Ma, *Chem. Eur. J.* **2007**, *13*, 3630.

